AGU PUBLICATIONS

Water Resources Research

RESEARCH ARTICLE
10.1002/2015WR018463

Key Points:
- Spatiotemporal variability in base flow $\delta^{18}O$ along two headwater streams
- Significant relationships between catchment structure and the range of base flow $\delta^{18}O$
- Patterns of base flow $\delta^{18}O$ unique to spatial arrangement of hillslopes along streams

Supporting Information:
- Supporting Information S1

Correspondence to:
N. Singh,
nksingh01@gmail.com

Citation:
Singh, N. K., R. E. Emanuel, and B. L. McGlynn (2016), Variability in isotopic composition of base flow in two headwater streams of the southern Appalachians, *Water Resour. Res.*, *52*, doi:10.1002/2015WR018463.

Received 4 DEC 2015
Accepted 11 MAY 2016
Accepted article online 17 MAY 2016

Variability in isotopic composition of base flow in two headwater streams of the southern Appalachians

Nitin K. Singh[1], Ryan E. Emanuel[1], and Brian L. McGlynn[2]

[1]Department of Forestry and Environmental Resources, North Carolina State University, Raleigh, North Carolina, USA, [2]Division of Earth and Ocean Sciences, Nicholas School of the Environment, Duke University, Durham, North Carolina, USA

Abstract We investigated the influence of hillslope scale topographic characteristics and the relative position of hillslopes along streams (i.e., internal catchment structure) on the isotopic composition of base flow in first-order, forested headwater streams at Coweeta Hydrologic Laboratory. The study focused on two adjacent forested catchments with different topographic characteristics. We used stable isotopes (^{18}O and ^{2}H) of water together with stream gauging and geospatial analysis to evaluate relationships between internal catchment structure and the spatiotemporal variability of base flow $\delta^{18}O$. Base flow $\delta^{18}O$ was variable in space and time along streams, and the temporal variability of base flow $\delta^{18}O$ declined with increasing drainage area. Base flow became enriched in ^{18}O moving along streams from channel heads to catchment outlets but the frequency of enrichment varied between catchments. The spatiotemporal variability in base flow $\delta^{18}O$ was high adjacent to large hillslopes with short flow paths, and it was positively correlated with the relative arrangement of hillslopes within the catchment. These results point to influence of unique arrangement of hillslopes on the patterns of downstream enrichment. Spatial variability in base flow $\delta^{18}O$ within the streams was relatively low during dry and wet conditions, but it was higher during the transition period between dry and wet conditions. These results suggest that the strength of topographic control on the isotopic composition of base flow can vary with catchment wetness. This study highlights that topographic control on base flow generation and isotopic composition is important even at fine spatial scales.

1. Introduction

Headwater streams constitute at least 70% of streams in the United States by length [*Leopold et al.*, 1964], and they exert strong control on hydrological and biogeochemical processes of downstream aquatic ecosystems. Headwater streams can be a major source of nutrients, organic matter, and sediments to higher order streams [*Gomi et al.*, 2002; *Alexander et al.*, 2007], and flow from these headwater streams serves as a significant source for drinking water, irrigation, and recreation for communities living downstream [*Freeman et al.*, 2007].

Understanding the spatiotemporal patterns of streamflow generation and their relationships with catchment structure, including topographic characteristics and spatial organization of hillslopes, remains one of the key challenges in catchment hydrology [e.g., *Beven*, 2006; *Payn et al.*, 2012]. Much research has focused on hydrological processes and responses associated with streamflow generation during storms, whereas streamflow generation during base flow conditions remains understudied by comparison [*Rodgers et al.*, 2005; *Tetzlaff and Soulsby*, 2008]. In general, base flow is the portion of precipitation that infiltrates the soil and recharges groundwater, gradually contributing to streamflow over relatively long durations [e.g., *Freeze*, 1974]. Base flow sustains perennial streams between precipitation events and during dry conditions. Base flow magnitude and composition directly influence stream habitat [e.g., *Boulton*, 2003], nutrient cycling [e.g., *Meyer and Wallace*, 2001], and overall functioning of headwater stream ecosystems [e.g., *Montgomery*, 1999] (see review by *Price* [2011]).

Stable isotopes of water (^{18}O, ^{2}H) are well-established tools for understanding sources, flow paths and residence times of natural waters at various spatial and temporal scales [*Sklash and Farvolden*, 1979; *McDonnell et al.*, 1991; *Rose*, 1996; *Weiler et al.*, 2003; *Jasechko et al.*, 2016]. Several studies have reported the isotopic composition of base flow across spatial scales and hydro-climatic regimes [e.g., *Bishop*, 1991; *Tetzlaff and*

Soulsby, 2008; *Laudon et al*., 2007; *Broxton et al*., 2009; *Brooks et al*., 2012; *Capell et al*., 2012; *Tekleab et al*., 2014]. In general, these studies provided insights into the longitudinal variability of sources, flow paths, and hydrologic processes that influence the formation of base flow at subcatchment or catchment scales (1–10^3 km^2). However, many of these studies focused on catchments dominated by a single, annual snowmelt event and its impacts on infiltration, storage, and base flow [cf. *Tetzlaff et al*., 2015].

Prior studies also revealed strong controls by topography on the isotopic composition of base flow [*McGlynn et al*. [2003]; *McGuire et al*. [2005]; *Rodgers et al*. [2005]; *Tetzlaff et al*. [2009]; *Asano and Uchida* [2012]; and *Heidbüchel et al*. [2013]. Key catchments-scale topographic characteristics affecting the isotopic composition of base flow in various hydro-climatic regimes include lengths and gradients of flow paths [*McGuire et al*., 2005; *Tetzlaff et al*., 2009; *Asano and Uchida*, 2012], slope angles and aspects [*Rodgers et al*., 2005; *Broxton et al*., 2009], drainage areas and densities [*Rodgers et al*., 2005; *Tetzlaff et al*., 2009, 2011], elevation [*Brooks et al*., 2012], and planform curvature [*Heidbüchel et al*., 2013]. Collectively, these studies inform our understanding of catchment-scale topographic controls on the isotopic composition of surface waters, with many of these studies focusing on snow-dominated regions, semiarid regions, and catchments ranging in size from (1–10^3 km^2).

In temperate, humid mountain regions, such as those of the southern Appalachian Mountains, first-order headwater catchments can be as small as 10 ha (0.1 km^2) in size, tend to be forested, and are minimally impacted, if at all, by snowmelt. In contrast to snow-dominated landscapes, base flow in this region derives from year-round precipitation. The hydrological processes that influence base flow generation in these rain-dominated regions can differ substantially from those in snow-dominated regions. It remains unknown whether the isotopic composition of base flow in these regions is controlled in the same manner by catchment-scale topography as in snow-dominated regions, semiarid regions, or at larger spatial scales. Moreover, additional work is needed to understand whether and how topographic variations within and among individual hillslopes, as well as the arrangement of hillslopes within a catchment, contribute to the isotopic composition of base flow.

The specific objectives of this study were to assess the spatiotemporal variability in the isotopic composition of base flow in two small (15 ha and 13 ha), forested headwater catchments and to quantify the role of internal catchment structure in mediating patterns of base flow ^{18}O. Here, we define internal catchment structure in two key ways: the distribution of topographic variables, including flow path lengths and gradients, within hillslopes, and the order in which different hillslopes are arranged along streams. We combined spatially dense sampling of stable isotopes (^{18}O, ^{2}H) in catchment waters with streamflow measurements and geospatial analysis, using a two-component mixing model to estimate the isotopic composition of lateral hillslope inflows along stream reaches. We use these results to assess links between topographic characteristics of hillslopes and observed patterns of stream water isotopes along two forested headwater streams during base flow conditions. This work addresses the following questions: (i) How does the isotopic composition of base flow vary in space and time along two first-order streams in the southern Appalachian Mountains? (ii) How do topographic characteristics of hillslopes relate to observed isotopic patterns, and are these patterns uniquely related to the arrangement of hillslopes within these catchments?

2. Study Site

Fieldwork was conducted at the Coweeta Hydrologic Laboratory (hereafter, Coweeta), a US Forest Service research station located in the southern Appalachian Mountains of western North Carolina, US (35°03′N, 83°25′W; Figure 1). Coweeta contains 26 gauged catchments covering a total of 21.85 km^2 and ranging in elevation from approximately 680–1500 m above mean sea level. Coweeta Creek, to which these catchments eventually drain, lies within the headwaters of the Tennessee River.

Coweeta's climate is classified as Marine and Humid Temperate under Köppen's climate system with frequent short duration precipitation events distributed year-round [e.g., *Swift et al*., 1988]. Mean annual precipitation is 1791 mm for the 75 year period 1937–2011, recorded at CS01, a low-elevation climate station near the US Forest Service (USFS) headquarters. Mean annual air temperature at CS01 is 12.6°C. Snow occasionally falls during the winter, but it is a minor component of the water balance. Soils in our study catchments are predominantly ultisols and inceptisols underlain by deeply weathered saprolite. The Coweeta basin has two major bedrock formations, both metamorphic - Tallulah Falls and the Coweeta Group

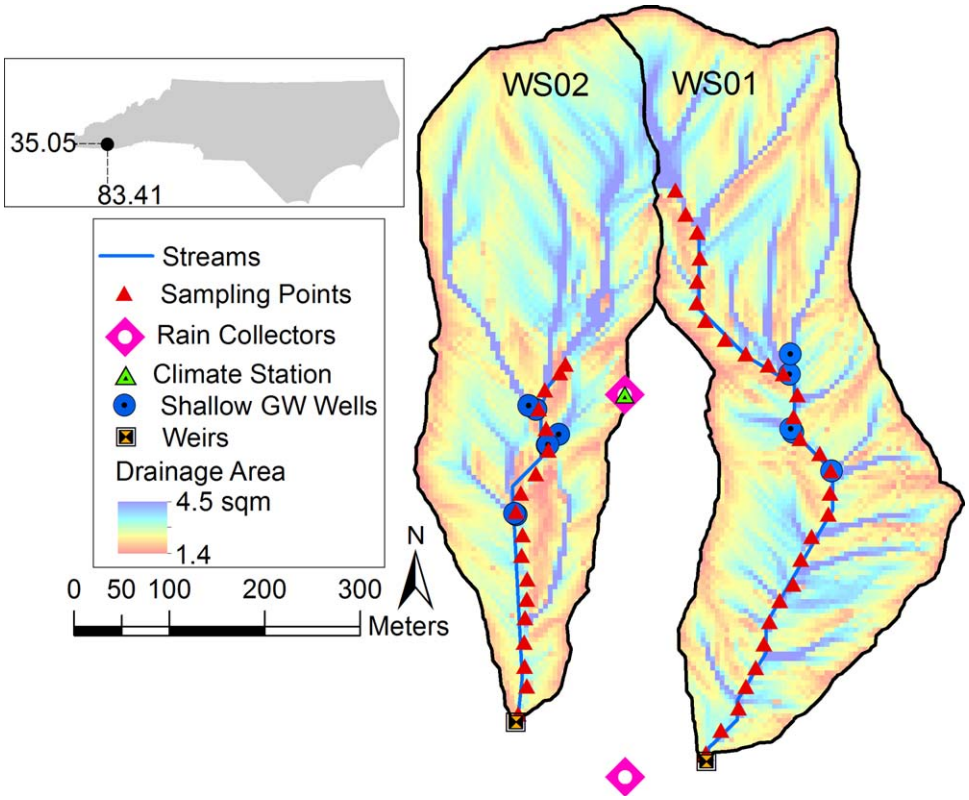

Figure 1. Catchments WS01 and WS02 showing streams, and sampling points together with instrumentation (shallow groundwater wells, rain collectors, weirs and climate station). Background shading shows drainage area (logarithmic scale). Inset shows the location of Coweeta Hydrologic Lab (Otto, North Carolina).

[*Hatcher*, 1971]. Tallulah Falls consists mostly of pelitic, schists and metavolcanic rocks. The Coweeta Group consists mainly of quartzites, gneisses, biotite, schists and metasandstones [*Hatcher*, 1974, 1979].

This study focused on two adjacent, south-facing catchments that include a broadleaf deciduous forest (WS02) and an evergreen coniferous forest (WS01) (Figure 1). The catchments are part of a long-term experiment evaluating effects of forest conversion on catchment water balances [*Swank and Douglass*, 1974]. WS02 was abandoned to secondary ecosystem succession around 1920 and serves as a reference for multiple paired catchment studies at Coweeta. WS01 was completely cleared in 1950 and replanted with white pine. Landscape characteristics for each catchment are summarized in Table 1. Both catchments share similar drainage areas, elevations, soils and bedrock geology. Additional details of watershed characteristics are presented in section 4.1.

3. Methods

3.1. Geospatial Analysis

Light detection and ranging (LIDAR) data were collected in 2010 by the National Center for Airborne Laser Mapping (NCALM). Data sets provided by NCALM included 1 m × 1 m digital elevation models (DEMs) of the bare earth surface and the top of the vegetation canopy. We resampled the 1 m × 1 m bare earth DEM to 10 m resolution to avoid the confounding effects of microtopography on geospatial algorithms used to estimate subsurface drainage patterns from surface topography [e.g., *Seibert and McGlynn*, 2007]. To delineate the stream network, we used a drainage area threshold of 2.8 ha, which closely matched our field measurements of channel head locations for each catchment. We used the multidirectional flow accumulation algorithm of *Seibert and McGlynn* [2007] to estimate the drainage area contributing to each 10 m pixel. Using the algorithms of *Grabs et al.* [2010] in SAGA GIS [*Böhneret al.*, 2008], we delineated hillslopes within each catchment, which were defined as the topographically delineated areas contributing to stream reaches between discrete sampling points. In the case of the channel head sampling point, the contributing

Table 1. Summary of Catchment Topographic Characteristics

Topographic Variables	WS01	WS02
Median elevation (m)	822	846
Median slope (°)	28	27
Median gradient to stream (m m^{-1})	0.43	0.40
Median flowpath length (m)	86	127
Median flowpath length/GTC[a] (m)	213	347
Median vegetation density (%)	99	99
Median vegetation height (m)	24	20
Aspect	South	South
Elevation range (m)	292	296
Perennial stream length (m)	700	411
Drainage area (ha)	15	13
Drainage density (km km^{-2})	4.7	3.2

[a]GTC = Gradient to Creek.

area was defined as the entire catchment area upstream of that point. Landscape variables computed at 10 m resolution included: elevation, slope, drainage area, flow path length to the stream, and gradient to creek (GTC). Later, we aggregated pixel-based topographic variables from both sides of the stream to obtain hillslope-scale median values contributing to the sampling points along the streams.

For each hillslope, defined as the local area contributing to the stream between sampling points, we used drainage area (DA) to compute hillslope size and incremental contributing area (ICA) with hillslope size (ΔDA) defined for each sampling point as

$$\Delta DA_x = DA_x - DA_{x+1} \quad (1)$$

where x represents a sampling point on the stream, x+1 is the next sampling point upstream, DA_x is the catchment drainage area for sampling point x, and DA_{x+1} is the catchment drainage area for sampling point x+1. We then computed ICA for each sampling point along stream as

$$ICA_x = \frac{\Delta DA_x}{DA_{x+1}} \quad (2)$$

where x and DA are defined following equation (1). We conceptualize ICA as a metric that describes the relative position of a hillslope within catchment and characterizes the capacity of an individual hillslope to alter the isotopic composition of stream water. Generally, hillslopes closer to the outlet have smaller ICA values than hillslopes closer to the headwaters. We posit that consideration of ICA is crucial to understanding individual and collective hillslope contributions to streamwater composition [*Jencso et al*., 2009; *Emanuel et al*., 2014]. This is because upstream drainage area, the denominator of equation (2), increases monotonically moving downstream. Although ICA values tend to decrease moving downstream, the decrease does not have to be monotonic since individual hillslopes can vary in size. Here, we confirmed that DA and ICA were not sensitive to the spatial resolution of the DEM by comparing results from analyses performed on 1 m, 5 m, and 10 m DEMs (Kruskal-Wallis, $p > 0.05$).

3.2. Hydrometric and Isotopic Measurements

The USFS has measured discharge continuously since 1934 at the outlet of each catchment using V-notch weirs. The month of February 2013 was marked by extremely wet conditions and extremely high and variable discharge observations, which were excluded from this analysis due to concerns about data quality. Climatological records for precipitation, air temperature and relative humidity have been measured by the USFS at climate stations near these catchments (CS01, CS21). The CS21 is located at an elevation of 817 m on a lateral ridge between the two study catchments, and CS01 is situated in a valley approximately 400 m away from the outlet of WS01 at an elevation of 685 m.

We sampled water from three sources: precipitation, base flow (i.e., stream water during base flow conditions), and shallow groundwater each month from June 2011 to June 2013 and analyzed samples for stable isotopes of water (^{18}O, ^{2}H; Figure 1). Base flow samples were collected along each of the two streams between each outlet and channel head. This sampling design was intended to capture a wide range of local stream and hillslope conditions within each catchment. We initially established sampling points every 25 m between the outlet and channel head of each stream, but we adjusted the spacing based on local geomorphology. For example, we moved sampling points to avoid splitting a single convergent hillslope between two sampling reaches. During each monthly sampling visit, base flow samples for each catchment were collected during a 2 h period on the same day. No detectable changes in runoff were noted at the catchment outlet during the 2 h periods.

Precipitation samples were collected in composite precipitation collectors located at the WS01 weir and at CS21 (Figure 1). Collectors were constructed from 10 cm diameter polycarbonate rain gauges protected against evaporation by foil-faced insulation on the outside and a thin (5–10 mm) layer of mineral oil inside. After sampling, precipitation collectors were cleaned and dried, and new mineral oil was added. Precipitation samples were collected every 1–4 weeks depending on the amount of precipitation. Total liquid water depth in the collector at the time of sampling was used to compute volume-weighted averages of precipitation ^{18}O and ^{2}H for each month. All precipitation isotopes are reported in volume-weighted values. Frozen precipitation samples were only encountered in January 2013 and were not included in the analysis.

Shallow groundwater was sampled monthly from 12 wells located across both catchments (Figure 1). In each catchment, three hillslopes of different sizes were instrumented with two wells each, a near-stream well and a hillslope well. Near stream wells were typically located 1–2 m away from the stream, whereas hillslope wells were sited on the toe of the hillslope up to a maximum distance of 18 m away from the stream thalweg [*Singh*, 2015]. Wells were constructed of 3.8 cm inner-diameter Poly vinyl chloride (PVC) conduit screened from approximately 10 cm below ground to the completion depth. Completion depths for all wells ranged from 0.9 to 3.5 m below the surface. Well screens were installed using a solid steel rod inserted into the screen and driven with a sledgehammer through soil and saprolite until refusal at the bedrock surface. A gas-powered auger whose bit matched the outer diameter of the PVC screening was used in some cases to probe for suitable locations. Bentonite clay was packed around each well at the soil surface to prevent surface runoff or direct precipitation from entering wells. Wells were purged prior to sampling and allowed to recharge. Samples were collected from the recharge water using a peristaltic pump (Geotech Environmental Equipment Inc., Denver, CO) with dedicated PVC sampling tubes installed in each well.

All water samples for isotopic analysis were collected in 20 mL high-density polyethylene (HDPE) vials sealed with a cone top cap to eliminate headspace and avoid isotopic fractionation. Samples were stored in a cool place until analyzed in the lab at the NC State University. At the time of analysis, samples were transferred to 2 mL glass vials and analyzed using a cavity ring down laser spectrometer (Model L2120i, Picarro Inc., Santa Clara, CA, ± 0.05 ‰). Isotopic compositions ($\delta^{18}O$) were reported in per mil (‰) relative to a standard as $\delta^{18}O = (R_{sample}/R_{std} - 1)*1000$, where R_{sample} and R_{std} are $^{18}O/^{16}O$ ratios for the sample and lab standards, respectively. Internal lab standards were calibrated against International Atomic Energy Agency standards, VSMOW2 (0 ‰ $\delta^{18}O$, 0 ‰ $\delta^{2}H$), GISP (-24.76 ‰ $\delta^{18}O$, -189.5 ‰ $\delta^{2}H$) and SLAP2 (-55.50 ‰ $\delta^{18}O$, -427.5 ‰ $\delta^{2}H$). We refer to a sample as enriched in ^{18}O relative to another sample if its $\delta^{18}O$ value is greater than that of the second sample [*Fry*, 2007]. We refer to a sample as depleted in ^{18}O relative to another sample if its $\delta^{18}O$ is less than the second sample. We assessed overall uncertainty in the isotopic analysis as the sum of accuracy (mean absolute difference between the measured and calibrated values of the duplicated blind unknown standards) and precision (mean standard deviation of the measured values of duplicated blind unknown standards). Total uncertainty was ± 0.14 ‰ for $\delta^{18}O$ and ± 1.76 ‰ for $\delta^{2}H$. Given the relatively large uncertainty in $\delta^{2}H$ compared to the range of values observed at Coweeta, $\delta^{2}H$ data were only used to develop a local meteoric water line and to assess the potential for evaporative enrichment of catchment waters. To quantify the pattern of increasing base flow $\delta^{18}O$ with distance downstream, we computed the slope and goodness of fit (r^2) for the relationship between base flow $\delta^{18}O$ and distance from the weir for each sampling date. In order to investigate the spatiotemporal patterns of base flow $\delta^{18}O$, we computed the mid-90th percentile range along sample reaches for both catchments.

3.3. Lateral Inflows of $\delta^{18}O$

We employed a simple mass balance approach to estimate $\delta^{18}O$ of net lateral inflows. The approach involved dilution gauging [*Day*, 1977] to develop an empirical relationship between drainage area and discharge combined with a linear mixing model of $\delta^{18}O$. Dilution gauging measurements were conducted during the months of June 2012, June 2013 and October 2013 (supporting information Figure S1), which cover relatively high and low base flow conditions. We used dilution gauging to estimate discharge at 50–100 m intervals along streams in both study catchments. Temperature and conductivity were measured using a conductivity probe (Model Professional Plus, YSI Inc., Ohio, US) positioned in the thalweg

of the stream and recording at 2 sec intervals. Discharge at a given location along a stream (Q_x) was calculated as

$$Q_x = \frac{M_t}{\int_0^t C(\tau)d\tau} \quad (3)$$

where $C(\tau)$ is the concentration [Cl^-] at location x for time variable τ starting at time 0 (time of tracer injection) and ending at t (time at which conductivity returns to the initial base value) and M_t is the mass of [Cl^-] injected into the stream. Each set of dilution gauging measurements lasted 10–14 h per catchment, and we used the continuous record of discharge at the outlet of each catchment to confirm that flow remained steady during each set of measurements.

The dilution gauging measurements were used to develop empirical power functions for each of the three sampling dates, relating drainage area at a point along the stream to the fraction of total discharge (Q) measured by the weir at the catchment outlet. Power functions took the form of equation (4)

$$\frac{Q_x}{Q} = m * (DA)^b \quad (4)$$

where DA is drainage area m and b are empirical coefficients. Coefficients m and b differed significantly among catchments, but they did not differ significantly between dates within a catchment (supporting information Figure S1). We combined the empirical power functions with daily discharge measured at the outlet weir to estimate daily discharge at each stream sampling point. An empirical function was assigned to each catchment on each sampling date based on the dilution gauging event whose discharge most closely matched discharge on the sampling date. For each stream reach, net lateral inflow was calculated as the difference between estimated discharge at the upstream and downstream end of each stream reach following equation (1).

We combined estimated discharge and $\delta^{18}O$ for each stream sampling point with estimated lateral inflow to compute the isotopic composition of net lateral inflow (L_x) from each hillslope to an individual sample reach as

$$L_x = \frac{Q_{x+1}C_{x+1} - Q_xC_x}{Q_{x+1} - Q_x} \quad (5)$$

where L is lateral inflow $\delta^{18}O$ (‰), C is base flow $\delta^{18}O$ (‰), Q is discharge (L s^{-1}) computed from equation (4), and indices x and x+1 represent upstream and downstream sampling points of a reach. We used the standard method [*Taylor*, 1982; *Genereux*, 1998] to estimate the uncertainty of lateral inflows $\delta^{18}O$ (hereafter, lateral $\delta^{18}O$) for each hillslope contributing to the sample reach for each set of monthly samples. Uncertainty of lateral $\delta^{18}O$ was computed for each hillslope for the entire study period. Hillslope area has some potential to confound our comparisons between lateral $\delta^{18}O$ and hillslope topographic characteristics, since hillslope area contributes implicitly to modeled lateral $\delta^{18}O$ through equation (4). However, given the weak or nonsignificant correlation between hillslope area and flow path length (refer to section 4.1 for details), a comparison of lateral $\delta^{18}O$ and hillslope-scale flow paths length still serves to elucidate the influence of landscape characteristics on base flow dynamics.

3.4. Assessing the Influence of Hillslope Arrangement

We used a model-data fusion approach [*See*, 2008] combined with Monte-Carlo simulation to test the influence of hillslope arrangement on observed patterns of base flow $\delta^{18}O$. Specifically, to test whether the relative arrangement of hillslopes within a catchment affected patterns of isotopic enrichment that we observed during some months, we randomized the arrangement of actual hillslopes within each catchment and simulated base flow $\delta^{18}O$ at each sampling point. For each catchment, we selected one month exhibiting relatively strong downstream enrichment of base flow ^{18}O: March 2012 for WS01 and April 2012 for WS02.

The Monte-Carlo simulation involved randomly permuting the positions of each catchment's hillslopes along its stream. For each hillslope, lateral discharge and $\delta^{18}O$ were prescribed based on observed conditions during the selected months. For each of 10,000 random permutations, we computed base flow $\delta^{18}O$ by resolving equation (5) for C_x and compared simulated base flow $\delta^{18}O$ to

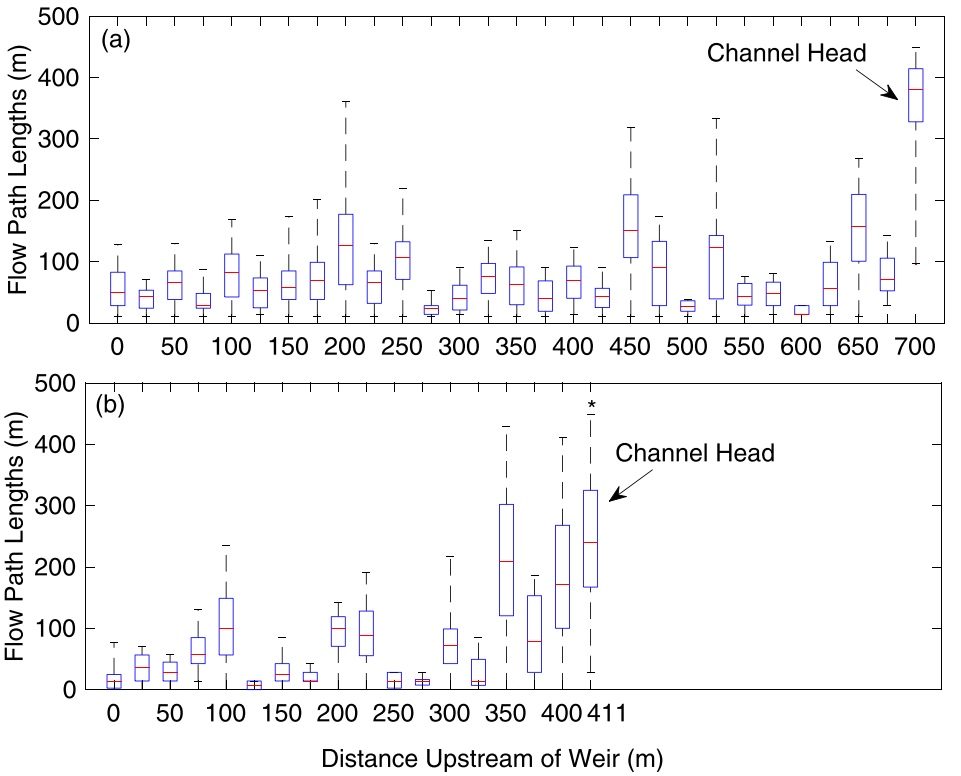

Figure 2. Boxplots showing distribution of flow path lengths for (a) WS01, and (b) WS02 (b). For each boxplot, upper and lower whiskers represent interquartile range and red line represents the median of the distribution. *Not to scale.

distance upstream of the weir using linear least squares regression. For each realization, we recorded the slope and goodness of fit (i.e., r^2) of the resulting regression between base flow $\delta^{18}O$ and distance upstream of the weir. Both test statistics were used to assess the enrichment patterns of base flow ^{18}O along the stream for each of the 10,000 realizations. Using a convex hull approach in MATLAB 13a (Mathworks Inc., Boston, MA), we estimated whether or not the slope and r^2 of the observed enrichment pattern fell within the 95% confidence interval of the bivariate distribution of 10,000 pairs of test statistics.

4. Results

4.1. Topographic Characteristics of Catchments and Hillslopes

In general, WS01 and WS02 share many similar topographic characteristics, including slope angles, aspects and drainage areas (Table 1). Differences emerge between WS01 and WS02 in other spatial variables, including flowpath lengths, stream lengths, and drainage density (Table 1). WS01 contains more dissected terrain than WS02, evident in the larger drainage density of WS01. Hillslopes in WS01 tend to be relatively small and uniform in area (mean hillslope area = 0.82, $\sigma^2 = 0.20$ ha) compared to hillslopes in WS02 (mean hillslope area = 0.92, $\sigma^2 = 0.59$ ha). Although the overall slope angles were similar for WS01 and WS02, hillslopes in WS01 were steeper than those in WS02 (Wilcoxon $p=0.02$). In both catchments, significant correlations were noted among several of the hillslope-scale topographic variables (supporting information Figure S2). For both WS01 and WS02, GTC was the only variable not correlated with any other topographic variable (supporting information Figure S2). Elevation was correlated to several topographic variables in WS02 but not WS01. Hillslope area was either weakly correlated with flow path length for WS01 or not correlated at all for WS02 (supporting information Figure S2).

Flow paths in WS01 were generally shorter than those in WS02. Median flow path lengths were significantly different between catchments (Wilcoxon $p<0.001$; Figure 2). Upper reaches of both catchments were generally adjoined by longer hillslopes than those found adjacent to reaches near the catchment outlets. We

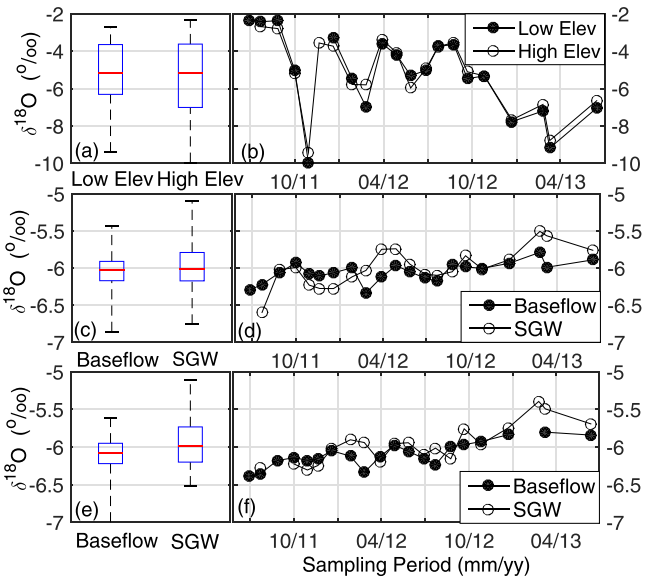

Figure 3. (a, b) Boxplots and time series of precipitation $\delta^{18}O$, base flow and (c, d) shallow groundwater (SGW) $\delta^{18}O$ for WS01; andbase flow (e, f) shallow groundwater (SGW) $\delta^{18}O$ for WS02. Boxplots show median (red), interquartile range (blue). Time series show low elevation (filled circle) and high elevation (open circle) for precipitation, or base flow (filled circle) and shallow groundwater (open circle) for WS01 and WS02. Error bars show uncertainty in the isotopic composition of each water source.

also found large spatial variability in the distribution of flow paths lengths along the hillslopes in the upper reaches of the catchments compared to lower reaches of the catchments (Figure 2).

4.2. Catchment Water Balance and Isotopic Compositions

The long-term climate station at Coweeta received a total of 3894 mm of precipitation from June 2011 to June 2013, or an average of 1869 mm yr^{-1}. January 2013 experienced 425 mm of precipitation, which was a single-month record for 81 years of data at CS01. Mean monthly precipitation at CS01 was 156 mm. For WS01 1170 mm of runoff occurred from June 2011 to June 2013, or an average of 511 mm yr^{-1} (1.40 mm d^{-1}). For WS02 1479 mm of runoff occurred during the study period, or an average of 715 mm yr^{-1} (1.96 mm d^{-1}). The difference in runoff between pine (WS01) and deciduous (WS02) catchments has been attributed to the phenological and eco-physiological differences between forest types in the two catchments [*Swank and Douglass*, 1974].

Precipitation $\delta^{18}O$ samples (n=46) showed high temporal variation at both low and high elevation sampling locations (Figure 3). Average monthly isotopic compositions were −5.02 ‰ and −5.16 ‰, for low and high elevations respectively. Neither the distributions of monthly precipitation $\delta^{18}O$ at high and low elevations nor their medians were significantly different according to a 2-sample Kolmogorov–Smirnov test ($p>0.05$) and a Wilcoxon rank-sum test ($p > 0.05$, Figure 3a). Similarly, monthly precipitation magnitude did not differ significantly between high-elevation and low-elevation rain gauges (Wilcoxon $p>0.05$). In addition to monthly samples, weekly precipitation $\delta^{18}O$ samples collected from June to August 2012 did not exhibit any significant elevation effect. Thus, we conclude that no significant elevation effects on the amount or isotopic composition of monthly precipitation existed during the course of this study. Although catchments at Coweeta are located in a relatively steep mountain terrain, the overall topographic relief in WS01 and WS02, about 290 m, is relatively small compared to other studies where significant gradients in precipitation magnitude or isotopic composition have been observed [e.g., *McGuire et al*., 2005; *Brooks et al*., 2012]. Given the lack of difference in either magnitude or isotopic composition between the two precipitation sampling locations, we believe that these data accurately characterize the variability in precipitation isotopes experienced by both catchments.

We used precipitation $\delta^{18}O$ and $\delta^{2}H$ to generate a local meteoric water line (LMWL) for the study period, which took the form $8.03*\delta\ ^{18}O+14$ (r^2 =0.95, supporting information Figure S3). The slope of the LMWL was similar to that of the global meteoric water line (GMWL) and representative of water vapor originating in humid environments [*Clark and Fritz*, 1997]. Catchment waters generally fell along or to the left of the LMWL and showed no sign of evaporative enrichment (supporting information Figure S3). During 2012 and 2013, 30 shallow (<60 cm) soil pore water samples collected periodically from five porous-cup lysimeters installed in WS02 did not show any evaporative enrichment relative to the LMWL (supporting information Figure S3).

In general, the isotopic composition of catchment waters differed significantly from that of precipitation. More specifically, precipitation was enriched in ^{18}O relative to both base flow and shallow groundwater. For

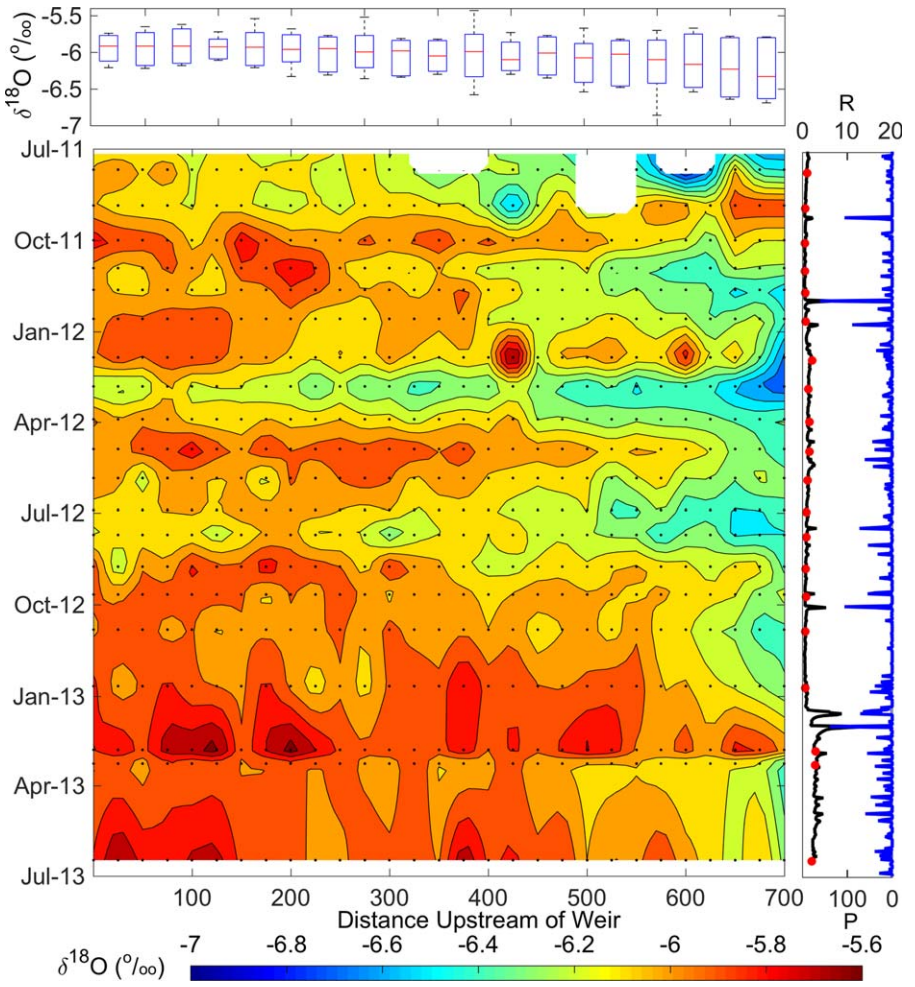

Figure 4. Interpolated contour plot of base flow $\delta^{18}O$ for 605 samples collected in WS01. Black dots show timing and location of discrete samples. Boxplots (above) show the temporal distribution of base flow $\delta^{18}O$ at each sampling point. Boxplot range is 5th to 95th percentile. Hydrograph (R) and hyetograph (P) for WS01 (right) shown with sampling dates in red. Units for both R and P are in mm d^{-1}.

the study period as a whole, median base flow $\delta^{18}O$ (WS01: -6.03 ‰; WS02: -6.08 ‰) was significantly different from median precipitation $\delta^{18}O$ for both catchments (Wilcoxon $p<0.05$; Figure 3). Streams in both catchments originated from perennial seeps that were depleted in ^{18}O relative to base flow sampled farther downstream.

More than 300 samples of shallow groundwater collected in WS01 and WS02 during the study period exhibited seasonal patterns in isotopic composition in which winter ^{18}O was relatively depleted compared to summer conditions (Figure 3). For both catchments, the medians of shallow groundwater $\delta^{18}O$ (WS01: -6.01 ‰; WS02: -5.98 ‰) were not significantly different from one another (Wilcoxon $p>0.05$). Shallow groundwater $\delta^{18}O$ was more variable than base flow $\delta^{18}O$ in both catchments during the study period (Figure 3).

Estimated lateral $\delta^{18}O$ from hillslopes had a median value of -5.89 ‰ for WS01 and a median value of -6.0 ‰ for WS02. Lateral inflows were depleted in^{18}O relative to precipitation (Wilcoxon $p < 0.05$) but lateral $\delta^{18}O$ was not significantly different from base flow $\delta^{18}O$ or shallow groundwater $\delta^{18}O$.

4.3. Spatiotemporal Patterns of Base Flow $\delta^{18}O$

Almost 1000 base flow samples collected along streams in WS01 and WS02 revealed unique patterns of $\delta^{18}O$, which were highly variable in space and time (Figures 4 and 5). In WS01, the temporal variability of base flow $\delta^{18}O$ declined significantly moving from the channel head to the outlet ($r=0.79$, $P<0.001$). In WS02, we observed greater temporal variability in base flow $\delta^{18}O$ than in WS01, but the strength of

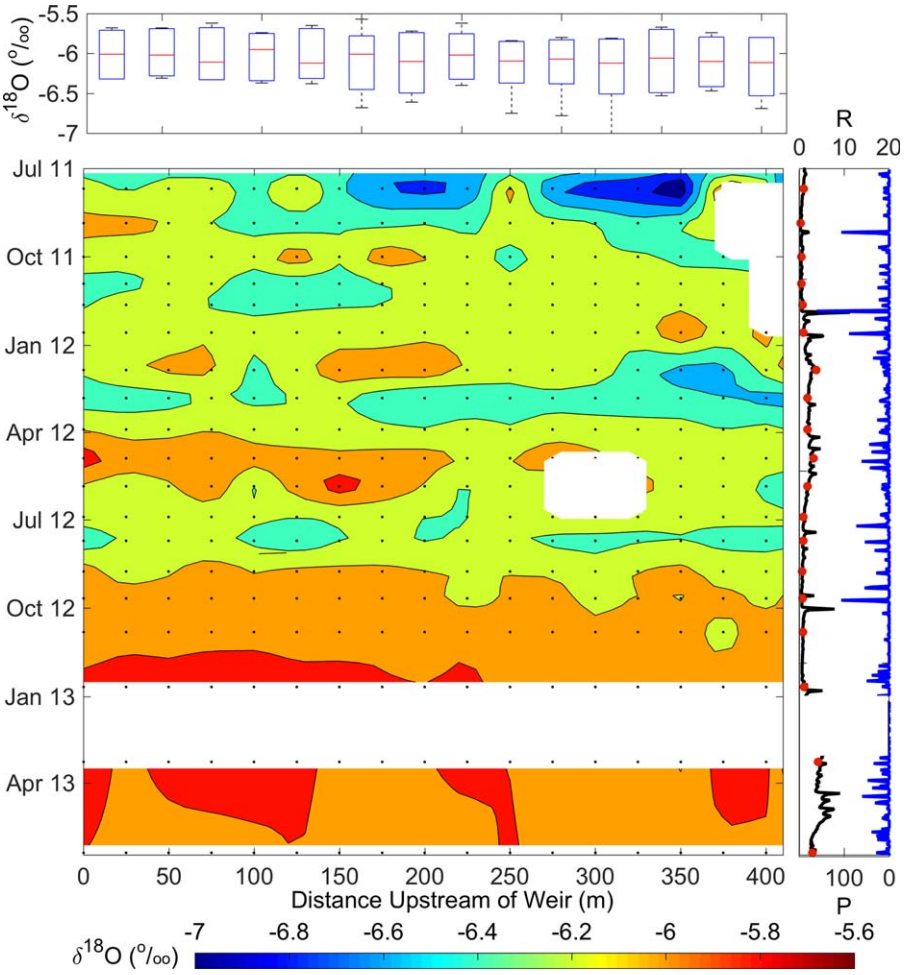

Figure 5. Interpolated contour plot of base flow $\delta^{18}O$ for 378 samples collected in WS02. Black dots show timing and location of discrete samples. Boxplots (above) show the temporal distribution of base flow $\delta^{18}O$ at each sampling point. Boxplot range is 5th to 95th percentile. Hydrograph (R) and hyetograph (P) for WS02 (right) shown with sampling dates in red. Units for both R and P are in mm d^{-1}.

declining pattern from the channel head to the outlet was weaker than in WS01 (r=0.59, P=0.02). We found a significant relationship between the temporal variability in base flow $\delta^{18}O$ and drainage area for WS01 (r=−0.76, P<0.001) and relatively weaker relationship for WS02 (r=−0.51, P=0.06; Figure 6). In both catchments, especially in the upstream-most reaches, we observed large temporal variability in base flow $\delta^{18}O$, with the mid-90th percentile of $\delta^{18}O$ for those reaches varying from 0.86 ‰ (WS01) to 0.93 ‰ (WS02).

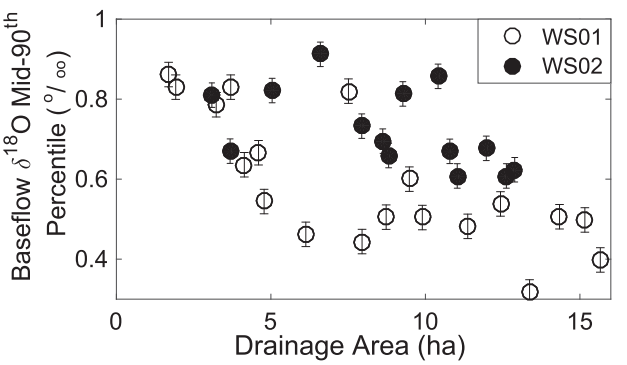

Figure 6. Mid-90th percentile of base flow $\delta^{18}O$ versus drainage area for WS01 and WS02. The correlation is significant for WS01 (r = −0.76, p<0.001). Error bars show uncertainty in the isotopic concentrations of base flow.

The patterns of base flow $\delta^{18}O$ along streams depended on the hydrologic conditions (i.e., the wetness state) of the catchment (Figure 7). In general, the spatial variability in base flow $\delta^{18}O$ was lower during both low flow and high flow conditions, and it was greater during the transition period between high and low flow conditions. During the driest months of the year (July, August, and September) base flow base flow $\delta^{18}O$ was relatively homogeneous within the stream and also indistinguishable from shallow groundwater $\delta^{18}O$ (Figures 3 and 5). As the catchments became wetter in the fall and

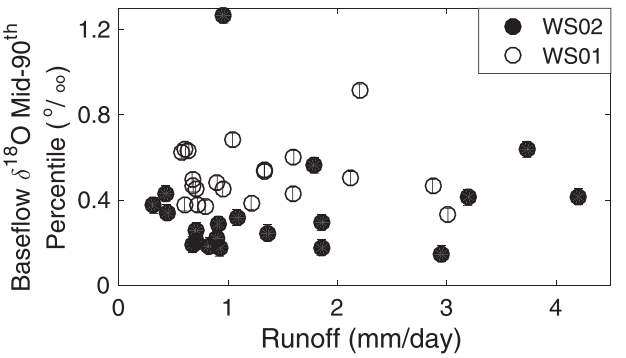

Figure 7. Mid-90th percentile of base flow $\delta^{18}O$ versus runoff for each sampling date in WS01 and WS02. Error bars show uncertainty in the isotopic concentrations of base flow.

winter (October to December), spatial variability in base flow $\delta^{18}O$ increased along the streams, but this pattern was more pronounced in WS01 than WS02 (Figures 4 and 5). After consecutive wet months, the overall spatial variability in base flow $\delta^{18}O$ was low, although base flow samples in reaches near the catchment outlet were enriched in ^{18}O relative to the channel head, especially in WS01. During wet periods (e.g., December 2012 to March 2013), base flow $\delta^{18}O$ was highly enriched in ^{18}O relative to rest of the sampling months. Furthermore, base flow $\delta^{18}O$ was almost identical to shallow groundwater $\delta^{18}O$ during these wet periods (Figures 3–5).

Generally, isotopic composition of base flow ^{18}O became enriched in ^{18}O along streams from the channel head to the outlet of each catchment. However, the strength of the relationship between base flow $\delta^{18}O$ and distance from the weir, quantified by slope and r^2 of least squares linear regression, varied from month to month (Table 2). Both catchments exhibited weak or no downstream enrichment of ^{18}O during wet periods, and significant correlations occurred more frequently in WS01 than in WS02.

4.4. Catchment Structure Controls on Base Flow $\delta^{18}O$ and Lateral Inflow $\delta^{18}O$

We identified relationships between the temporal variability in base flow $\delta^{18}O$ for a sampling reach and the corresponding ICA within each catchment (Figure 8). We also found that the sample reaches with the greater temporal variability in base flow $\delta^{18}O$ were flanked by hillslopes (approximately 1 ha) with high ICA values and more internal variability in flow path lengths (Figures 2 and 4, and 8). Some of the samples reaches (e.g., 425 m in WS01, 325 m in WS02; Figures 2 and 4) that exhibited more temporal variability in base flow $\delta^{18}O$ were adjoined by large but steep hillslopes (i.e., small ratio of flow path length to GTC).

Table 2. Relationship Between Base Flow $\delta^{18}O$ and the Distance From Channel Head to the Catchment Outlet

	WS01		WS02	
Date	r^2	Slope[a]	r^2	Slope[a]
2011/06	0.77	−0.07		
2011/07	0.40	−0.06		
2011/08				
2011/09	0.47	−0.03	0.58	−0.07
2011/10	0.55	−0.06	0.46	−0.05
2011/11	0.67	−0.07		
2012/12	0.74	−0.05		
2012/01				
2012/02	0.68	−0.06	0.51	−0.04
2012/03	0.73	−0.05		
2012/04	0.52	−0.05	0.84	−0.08
2012/05	0.46	−0.03		
2012/06	0.75	−0.06		
2012/07	0.52	−0.04		
2012/08	0.53	−0.04	0.33	−0.02
2012/09	0.69	−0.04	0.34	−0.03
2012/10	0.61	−0.05		
2012/12			0.87	−0.08
2013/02				
2013/03	0.51	−0.04		
2013/06	0.55	−0.04		

[a]Units: ‰ (100 m)$^{-1}$.
[b]Blank spaces indicate "Not significant at $\alpha = 0.05$."

The estimated $\delta^{18}O$ values of lateral inflows were indistinguishable from precipitation for all but the largest hillslopes. In particular, hillslopes larger than 1 ha with median flow paths longer than 150 m had estimated values of lateral $\delta^{18}O$ that were significantly depleted in ^{18}O relative to precipitation ^{18}O (Figure 9). Lateral $\delta^{18}O$ estimates for individual months and hillslopes exhibited large uncertainties (>2 ‰) that were inversely proportional to hillslope size and related to our method for estimating lateral $\delta^{18}O$ (equation (4)). These large uncertainties prevented us from assessing the significance of topographic influences on monthly estimates of lateral $\delta^{18}O$.

Test statistics (slope and r^2) obtained from the Monte-Carlo simulation showed that the observed

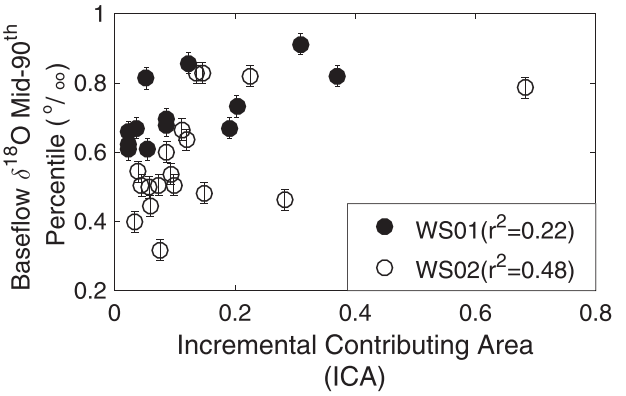

Figure 8. Mid-90th percentile of base flow δ^{18}O versus incremental contributing area (ICA) for WS01 and WS02. Error bars show uncertainty in the isotopic concentrations of base flow.

patterns of downstream ^{18}O enrichment, characterized by least squares linear regression slope and r^2, cannot be replicated by randomizing the arrangement of actual hillslopes within a watershed (Figure 10). For WS01, the observed slope of -0.05 ‰ (100 m)$^{-1}$ and r^2 of 0.73 fell outside of the 95% confidence interval of the bivariate distribution of r^2 and slope for randomly arranged hillslopes (median $r^2 = 0.11$, median slope $= -0.04$ ‰ (100 m)$^{-1}$). For WS02, the observed slope of -0.08 ‰ (100 m)$^{-1}$ and r^2 of 0.84 fell at about the 88th percentile of the bivariate distribution of r^2 and slope for randomly arranged hillslopes (median $r^2 = 0.30$, median slope $= -0.06$ ‰ (100 m)$^{-1}$).

5. Discussion

5.1. How do Hydrologic Conditions Affect the Spatiotemporal Variability of Base Flow δ^{18}O?

Our results suggest that the observed variability in base flow δ^{18}O is due in part to hydrologic conditions, which is to say that the wetness state of the catchments at different times of the year influences the isotopic composition of base flow (Figure 7). During drier months (July, August, and September), base flow δ^{18}O was more homogenous and similar to the mean value of shallow groundwater δ^{18}O in the catchments. During drier months with lower rates of base flow discharge, many hillslopes were likely hydrologically disconnected from the stream channel, leaving only a small fraction of the catchment contributing actively to base flow in the stream [e.g., *Jencso et al*., 2009; *Nippgen et al*., 2015].

As the catchments transitioned from dry to wet, base flow δ^{18}O became more variable along each of the streams. This increasing variability during the dry-to-wet transition may reflect nonuniform expansion of the connected catchment area contributing actively to base flow in the stream [*Nippgen et al*., 2015; *Soulsby et al*., 2015]. It is likely that hillslopes with different isotopic signatures activate at different times during the wet-up period and may contribute to an increase in observed spatial variability of base flow δ^{18}O. During the wettest times of the year (e.g., February, March), both base flow and shallow groundwater became enriched in ^{18}O (Figures 3 and 4). The simultaneous enrichment of base flow ^{18}O and shallow groundwater ^{18}O during these months suggests that large amounts of existing shallow groundwater were replaced by new precipitation, which tends to be enriched in ^{18}O relative to other catchment waters. Thus, our results support the classic conceptual model of translatory flow proposed for these catchments by *Hewlett and Hibbert* [1967], but only during the wettest times of the year.

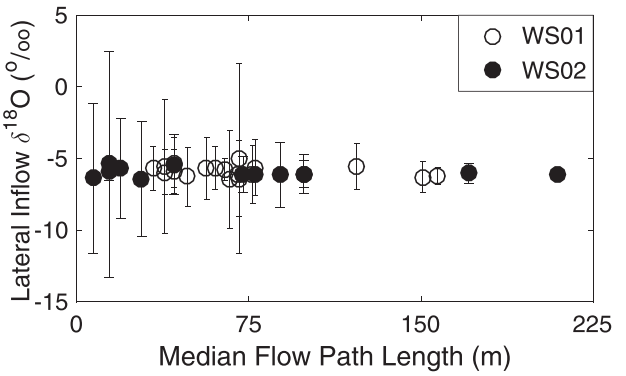

Figure 9. Median of lateral inflow δ^{18}O organized by each hillslope's corresponding flow path lengths for WS01 and WS02. Error bar represents uncertainty in lateral inflow δ^{18}O.

These results are consistent with other studies that have reported links between wetness and hydrologic connectivity within catchments and observed patterns of base flow δ^{18}O [*Rodgers et al*., 2005; *Heidbüchel et al*., 2013; *Soulsby et al*., 2015]. In particular, *Heidbüchel et al*. [2013] showed that relationships between base flow δ^{18}O and several catchment spatial characteristics depended upon wetness state. *Soulsby et al*. [2015] demonstrated that patterns of base flow δ^{18}O are controlled in part by hydrological

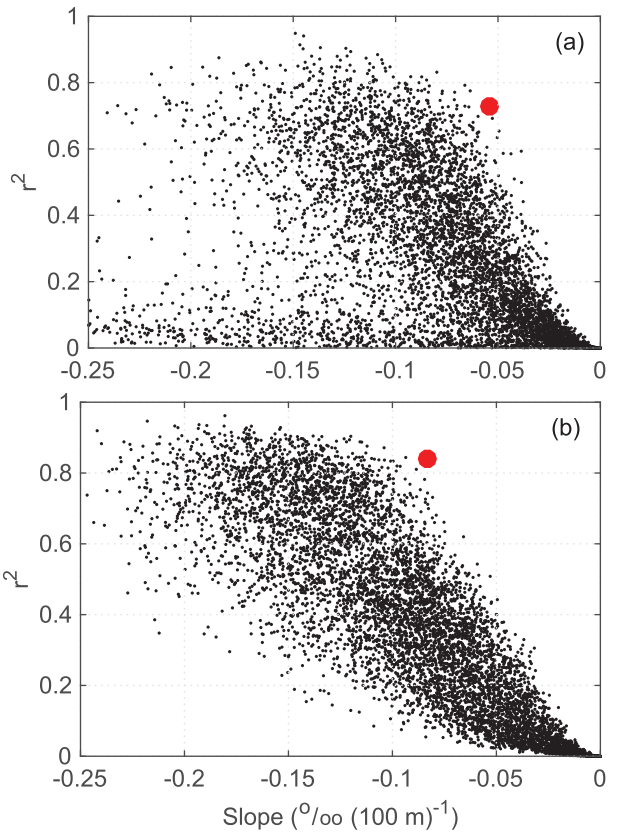

Figure 10. Coefficient of determination (r^2) and regression slope for observed downstream ^{18}O enrichment (red) and 10,000 random simulations of hillslope arrangements (black) for (a) WS01 and (b) WS02. Observed conditions correspond to March 2012 for WS01 and April 2012 for WS02.

connectivity between landscapes and streams. Our work contributes to the growing body of research demonstrating the influence of hydrologic conditions on patterns of base flow $\delta^{18}O$.

Few studies have documented patterns of base flow $\delta^{18}O$ at the spatial and temporal scales presented here. In a larger (187 km^2) forested catchment in Georgia (USA), *Rose* [1996] found a range of 2.3 ‰ (n=24) for base flow $\delta^{18}O$ between the weir and channel head over a 2 year period. *Rodgers et al.* [2005] sampled base flow $\delta^{18}O$ on a weekly basis at the weirs of six catchments that varied in size from 1.3 km^2 to 233 km^2 and represented different type of land use, soil, and geology in northeastern Scotland. They found base flow $\delta^{18}O$ ranges of 1.70 ‰ to 3.2 ‰ (n not given), and similar ranges were observed by *Tetzlaff and Soulsby* [2008] in the same region. *Broxton et al.* [2009] found base flow $\delta^{18}O$ ranges of about 2 ‰ (n=134) for 15 catchments in New Mexico varying in size from 0.1 to 14 km^2. The base flow $\delta^{18}O$ range of 1.4 ‰ (n=983) that we observed at Coweeta was of similar magnitude to the ranges reported by other studies, despite the relatively small size of Coweeta catchments. These results suggest that even very small (<1 km^2) headwater catchments exhibit considerable heterogeneity in hydrological processes influencing base flow.

5.2. How do the Structure and Arrangement of Hillslopes Within Catchments Affect Base Flow $\delta^{18}O$?

We observed significant relationships between spatial and temporal measures of base flow $\delta^{18}O$ variability and internal catchment structures (Figures (6 and 8), and 10). In general, internal catchment structures variables such as the flow path length, gradient to creek [e.g., *McGuire et al.*, 2005], and drainage area, can influence patterns of base flow $\delta^{18}O$ by altering the delivery time (i.e., residence time) or the amount of water entering the stream as base flow. Other studies have indicated that the temporal variability of stream $\delta^{18}O$ can be related to the age or residence time of water [*Rodhe et al.*, 1996; *Tetzlaff et al.*, 2009; *Asano and Uchida*, 2012]. Other studies link the ratio between flow path length and GTC to hydraulic gradients, which influence the rate of movement of subsurface flow [*Jencso and McGlynn*, 2011], and are positively correlated with residence times of water [e.g., *McGuire et al.*, 2005]. In other words, the smaller the ratio of flow path length to GTC, the shorter the residence time. In our study catchments, the ratio of flow path lengths to GTC and flow path length are highly correlated (supporting information Figure S2). Thus, the large temporal variability observed in base flow $\delta^{18}O$ for some sample reaches adjoined by hillslopes with short median flowpaths (e.g., WS01, 425 m and WS02 250 m in Figure 2) could be attributed to short residence times of water along these hillslopes.

Figure 8 revealed dependence of base flow $\delta^{18}O$ on ICA, which describes the relative location of a hillslope within a watershed and a hillslope's capacity to influence the stream's isotopic composition. To alter the stream's isotopic composition, the adjacent hillslope must be large enough to produce sufficient amount of lateral flow, and the isotopic composition of that water must differ substantially from water already in the stream. Due to relatively low flow in upstream reaches near the channel head, it is easier for hillslopes along

these reaches to alter stream isotopic composition than it is for downstream hillslopes where flows are greater. This effect, which is also described by equation (4), may explain the large variability in base flow δ^{18}O observed in the upstream reaches compared to downstream reaches.

Lateral inflow δ^{18}O was less variable for hillslopes with long flow paths (median flow path $>$ 150 m) and fell within the range of observed base flow δ^{18}O (Figures 3 and 9). The reduced variability in lateral δ^{18}O may be attributed to greater storage on these large hillslopes [e.g., *Tetzlaff et al*., 2014]. Conversely, smaller hillslopes with relatively short flow paths would have less capacity to store water and dampen the precipitation δ^{18}O signal through mixing. Smaller hillslopes might transmit precipitation δ^{18}O signals more readily than larger hillslopes, but it could be more difficult for them to influence base flow in the stream unless they are located close to the channel head.

Our Monte-Carlo simulation of hillslope arrangement further demonstrates the importance of catchment structure on patterns of base flow δ^{18}O. In particular, our results show that the actual arrangement of hillslopes within each of the two catchments produces a pattern of base flow δ^{18}O enrichment from the channel head to the outlet that cannot be reproduced by a random arrangement of the same hillslopes (Figure 10). These simulation results demonstrate that observed patterns in base flow δ^{18}O enrichment are intimately linked to the unique arrangement of hillslopes in the study catchments. Each hillslope possesses a unique combination of several topographic characteristics (e.g., length of flow paths, flow path gradient), and has a unique ability to alter the isotope composition of base flow in its adjoining reach, depending upon internal characteristics of the hillslope and its relative position within the catchment. In particular, the overall arrangement of hillslopes within a catchment determines the ICA of each hillslope, which is an indicator of the hillslope's ability to alter the isotopic composition of base flow (Figure 8). Because of the connection between hillslope order and ICA, random arrangement of the same hillslopes can yield different patterns of downstream isotopic enrichment, including no significant enrichment whatsoever (Figure 10). Effectively, there is a degree of determinism in the arrangement of hillslopes within a catchment and the evolving isotopic composition of downstream waters. Overall, these results indicate that internal catchment structure, including the arrangement of hillslopes within a headwater catchment can influence patterns of base flow δ^{18}O. These results support a growing body of work suggesting that hydrologic response is inextricably linked to catchment structure [e.g., *McGuire et al*., 2005; *Broxton et al*., 2009; *Capell et al*., 2012; *Heidbüchel et al*., 2013].

5.3. Implications

Using stable isotopes of water (^{18}O), this study advances our understanding of how streamflow varies in space and time by extending observations from the catchment outlet into the catchment itself (Figures 4 and 5). Our results corroborate previous findings that streamflow responses measured at a catchment outlet may not accurately represent the complexity of upstream processes [*McGlynn et al*., 2004].

Our results have implications for isotope-based hydrograph separation techniques, which generally assume that base flow is homogenous in space within a catchment [cf., *Buttle*, 1994]. We illustrate this using a two-component based hydrograph separation method [e.g., *Genereux*, 1998; cf. *Genereux and Hooper*, 1998], to estimate percentage change in the fraction of old water to new water for base flow δ^{18}O values measured at catchment outlet (-5.91 ‰) and channel head (-6.63 ‰) for the month of January 2012 in WS01. Based on our observation, we use representative values of stream δ^{18}O and precipitation δ^{18}O, -5.12 ‰ and -5 ‰, respectively. Our results suggest that the fraction of old to new water was 47% higher for the isotopic composition of base flow measured at catchment outlet than the channel head. Although we acknowledge that the magnitude of change in the fraction of old to new water can be sensitive to precipitation δ^{18}O and stream δ^{18}O that we used in the analysis. These results suggest minor differences in base flow δ^{18}O can drastically alter the hydrograph separation results and encourage caution in applying isotope-based hydrograph separation methods in small headwater catchments such as these.

These results also help elucidate the role of hillslopes in mediating spatial patterns of base flow through time within a catchment. Our work shows that both hillslope characteristics and their arrangement within a catchment can influence streamflow generation during base flow conditions. It complements other work linking topographic controls to hillslope-stream connectivity [*Jencso et al*., 2009] and linking connectivity to water quality [*McGlynn and McDonnell*, 2003; *Pacific et al*., 2010]. Recognizing topographic and other structural controls on streamflow composition also has the potential to advance our understanding of solute

concentrations and their export from headwater catchments, possibly aiding identification of biogeochemical hotspots and sources of pollutants [*Kimball et al*., 2010].

6. Conclusions

We reported the isotopic composition of precipitation, base flow and shallow groundwater in two small headwater catchments of the southern Appalachian Mountains, collected over a 2 year period. Our analysis of nearly 1000 base flow samples revealed significant spatiotemporal variability in base flow δ^{18}O within relatively small (15 ha and 13 ha), forested headwater catchments. We link this variability in base flow δ^{18}O to hydrologic conditions experienced during the 2 year study, to topographic characteristics of catchments and their hillslopes, and to the specific arrangement of hillslopes within each catchment.

The relationship between ICA and the temporal range of base flow δ^{18}O suggests that catchment structure influences patterns of base flow for these first-order mountain streams. Weak or nonexistent linear trends in base flow δ^{18}O along streams during extreme wet and dry conditions and relatively strong linear trends during intermediate conditions indicate that structural controls on base flow δ^{18}O are sensitive to hydrologic conditions within the catchment. Analysis of lateral inflow δ^{18}O highlighted the important role of large hillslopes with long flow paths in dampening precipitation δ^{18}O before releasing it to the stream. Overall, these results further confirm and add to our fundamental understanding of intimate linkages between catchment structure and base flow generation for small headwater catchments. This work further emphasizes the utility of stable isotopes for understanding spatial and temporal patterns of base flow at high spatial resolution.

Acknowledgments
This work was funded by the Department of Forestry and Environmental Resources at North Carolina State University and by NSF Awards EAR-0838193 (Emanuel) DEB-0823293, (Emanuel), and EAR-0837937 (McGlynn). Singh received support from a Global Change Fellowship from the US Department of Interior Southeast Climate Science Center, from a Geological Society of America Student Research Grant, and from a North Carolina Association of Environmental Professionals Student Research Grant. Kelsey Jencso, Fabian Nippgen and Ruchi Bhattacharya provided vital support and enabled collection of field data sets. The US Forest Service Coweeta Hydrologic Laboratory provided access to field sites and supporting data sets. Water isotope and dilution gaging data used in this paper can be requested from the NCSU Ecohydrology and Watershed Science Group using contact information found at go.ncsu.edu/ecohydrology. Streamflow and climate data can be requested from the USDA Forest Service, and Lidar data can be accessed at opentopography.org.

References

Alexander, R. B., E. W. Boyer, R. A. Smith, G. E. Schwarz, and R. B. Moore (2007), The role of headwater streams in downstream water quality, *J. Am. Water Resour. Assoc.*, *43*, 41–59, doi:10.1111/j.1752-1688.2007.00005.x.

Asano, Y., and T. Uchida (2012), Flow path depth is the main controller of mean base flow transit times in a mountainous catchment, *Water Resour. Res.*, *48*, W03512, doi:10.1029/2011WR010906.

Beven, K. (2006), Commentary, in *Streamflow Generation Processes*, edited by K. Beven, pp. 1–431, IAHS Press, Wallingford, U. K.

Bishop, K. H. (1991), Episodic increases in stream acidity, catchment flow pathways and hydrograph separation, PhD thesis, Univ. of Cambridge, U. K.

Böhner, J., T. Blaschke, and L. Montanarella (Eds.) (2008), *SAGA: System for an Automated Geographical Analysis*, 113 pp., Inst. of Geogr., Univ. of Hamburg, Hamburg, Germany.

Boulton A. J. (2003), Parallels and contrasts in the effects of drought on stream macroinvertebrate assemblages, *Freshwater Biol.*, *48*(7), 1173–1185.

Brooks R. J., P. J. Wigington Jr., D. L. Phillips, R. Comeleo, and R. Coulombe (2012), Willamette River Basin surface water isoscape (δ^{18}O and δ^{2}H): Temporal changes of source water within the river, *Ecosphere*, *3*, art39, doi:10.1890/ES11-00338.1.

Broxton, P. D., P. A. Troch, and S. W. Lyon (2009), On the role of aspect to quantify water transit times in small mountainous catchments, *Water Resour. Res.*, *45*, W08427, doi:10.1029/2008WR007438.

Buttle, J. M. (1994), Isotope hydrograph separation and rapid delivery of pre-event water from drainage basins, *Prog. Phys. Geogr.*, *18*(1), 16–41.

Capell, R., D. Tetzlaff, A. J. Hartley, and C. Soulsby (2012), Linking metrics of hydrological function and transit times to landscape controls in a heterogeneous mesoscale catchment, *Hydrol. Processes*, *26*(3), 405–420.

Clark, I. D., and P. Fritz (1997), *Environmental Isotopes in Hydrogeology*, 328 pp., CRC Press, Boca Raton, Fla.

Day, T. J. (1977), Field procedures and evaluation of a slug dilution gauging method in mountain streams, *J. Hydrol.*,*16*(2), 113–133.

Emanuel, R. E., A. G. Hazen, B. L. McGlynn, and K. G. Jencso (2014), Vegetation and topographic influences on the connectivity of shallow groundwater between hillslopes and streams, *Ecohydrology*, *7*(2), 887–895.

Freeman, C. M., C. M. Pringle, and C. R. Jackson (2007), Hydrologic connectivity and the contribution of stream headwaters to ecological integrity at regional scales, *J. Am. Water Resour. Assoc.*, *43*, 5–14.

Freeze R. A. (1974), Streamflow generation, *Rev. Geophys.*, *12*(4), 627–647.

Fry, B. (2007), *Stable Isotope Ecology*, Springer Science & Business Media, N. Y.

Genereux, D. (1998), Quantifying uncertainty in tracer-based hydrograph separations, *Water Resour. Res.*, *34*(4), 915–919.

Genereux, D. P., and R. P. Hooper (1998), Oxygen and hydrogen isotopes in rainfall-runoff studies, in *Isotope Tracers in Catchment Hydrology*, edited by C. Kendall and J. J. McDonnell, pp. 319–346, Elsevier Sci., N. Y.

Gomi, T., R. C. Sidle, and J. S. Richardson (2002), Understanding processes and downstream linkages of headwater systems headwaters differ from downstream reaches by their close coupling to hillslope processes, more temporal and spatial variation, and their need for different means of protection from land use, *BioScience*, *52*(10), 905–916.

Grabs, T. J., K. G. Jencso, B. L. McGlynn, and J. Seibert (2010), Calculat- ing terrain indices along streams: A new method for separating stream sides, *Water Resour. Res.*, *46*, W12536, doi:10.1029/2010WR009296.

Hatcher, R. D., Jr. (1971), Geology of Rabun and Habesham counties, Georgia: A reconnaissance study, *Georgia Geol. Surv. Bull.*, *83-A*, 1–48.

Hatcher, R. D., Jr. (1974), Introduction to the tectonic history of northeast Georgia, *Geol. Surv. Guideb.*, *13-A*, 1–59.

Hatcher R. D., Jr. (1979), The Coweeta Group and Coweeta syncline: Major features of the North Carolina-Georgia Blue Ridge, *Southeast Geol.*, *21*(1), 17–29.

Heidbüchel, I., P. A. Troch, and S. W. Lyon (2013), Separating physical and meteorological controls of variable transit times in zero-order catchments, *Water Resour. Res.*, *49*, 7644–7657, doi:10.1002/2012WR013149.

Hewlett, J. D., and A. R. Hibbert (1967), Factors affecting the response of small watersheds to precipitation in humid areas, *For. Hydrol.*, *1*, 275–290.
Jasechko, S., J. W. Kirchner, J. M Welker, and J. J. McDonnell (2016), Substantial proportion of global streamflow less than three months old, *Nat. Geosci.*, 9, 126–129.
Jencso, K. G., and B. L. McGlynn (2011), Hierarchical controls on runoff generation: Topographically driven hydrologic connectivity, geology, and vegetation, *Water Resour. Res.*, *47*, W11527, doi:10.1029/2011WR010666.
Jencso, K. G., B. L. McGlynn, M. N. Gooseff, S. M. Wondzell, K. E. Bencala, and L. A. Marshall (2009), Hydrologic connectivity between landscapes and streams: Transferring reach- and plot-scale understanding to the catchment scale, *Water Resour. Res.*, *45*, W04428, doi:10.1029/2008WR007225.
Kimball, B. A., R. L. Runkel, and K. Walton-Day (2010), An approach to quantify sources, seasonal change, and biogeochemical processes affecting metal loading in streams: Facilitating decisions for remediation of mine drainage, *Appl. Geochem.*, *25*, 728–740.
Laudon, H., V. Sjöblom, I. Buffam, J. Seibert, and M. Mörth (2007), The role of catchment scale and landscape characteristics for runoff generation of boreal streams, *J. Hydrol.*, *344*(3), 198–209.
Leopold, L. B., M. G. Wolman, and J. P. Miller (1964), *Fluvial Processes in Geomorphology*, 522 pp., W. H. Freeman, San Francisco, Calif.
McDonnell, J. J., M. K. Stewart, and I. F. Owens (1991), Effects of catchment-scale subsurface watershed mixing on stream isotopic response. *Water Resour. Res.*, *27*(12), 3065–3073.
McGlynn, B. L., and J. J. McDonnell (2003), Role of discrete landscape units in controlling catchment dissolved organic carbon dynamics, *Water Resour Res.*, *39*(4), 1090, doi:10.1029/2002WR001525.
McGlynn, B. L., J. J. McDonnell, J. Seibert, and M. K. Stewart (2003), On the relationships between catchment scale and streamwater mean residence time, *Hydrol. Processes*, *17*, 175–181.
McGlynn, B. L., J. J. McDonnell, J. Seibert, and C. Kendall (2004), Scale effects on headwater catchment runoff timing, flow sources, and groundwater-streamflow relations, *Water Resour. Res.*, *40*, W07504, doi:10.1029/2003WR002494.
McGuire, K. J., J. J. McDonnell, M. Weiler, C. Kendall, B. L. McGlynn, J. M. Welker, and J. Seibert (2005), The role of topography on catchment-scale water residence time. *Water Resour. Res.*, *41*, W05002, doi:10.1029/2004WR003657.
Meyer, J. L., and J. B. Wallace (2001), Lost linkages and lotic ecology: Rediscovering small streams, in *Ecology: Achievement and Challenge*, edited by M. Press, N. Huntly, and S. Levin, chap. 14, pp. 295–317, Blackwell Sci., Oxford, U. K.
Montgomery D. R. (1999), Process domains and river continumm, *J. Am. Water Resour. Assoc.*, *35*(2), 397–410.
Nippgen, F., B. L. McGlynn, and R. E. Emanuel (2015), The spatial and temporal evolution of contributing areas. *Water Resour. Res.*, *51*, 4550–4573, doi:10.1002/2014WR016719.
Pacific, V. J., K. G. Jencso, and B. L. McGlynn (2010), Variable flushing mechanisms and landscape structure control stream DOC export during snowmelt in a set of nested catchments, *Biogeochemistry*, *99*(1-3), 193–211.
Payn, R. A., M. N. Gooseff, B. L. McGlynn, K. E. Bencala, and S. M. Wondzell (2012), Exploring changes in the spatial distribution of stream baseflow generation during a seasonal recession, *Water Resour. Res.*, *48*, W04519, doi:10.1029/2011WR011552.
Price, K. (2011), Effects of watershed topography, soils, land use, and climate on baseflow hydrology in humid regions: A review, *Prog. Phys. Geogr.*, *35*(4), 465–492, doi:10.1177/0309133311402714.
Rodgers, P., C. Soulsby, S. Waldron, and D. Tetzlaff (2005), Using stable isotope tracers to assess hydrological flow paths, residence times and landscape influences in a nested mesoscale catchment, *Hydrol. Earth Syst. Sci.*, *9*(3), 139–155.
Rodhe, A., L. Nyberg, and K. Bishop (1996), Transit times for water in a small till catchment from a step shift in the oxygen 18 content of the water input. *Water Resour. Res.*, *32*(12), 3497–3511.
Rose, S. (1996), Temporal environmental isotopic variation within the Falling Creek (Georgia) catchment: Implications for contributions to streamflow, *J. Hydrol.*, *174*, 243 261.
See, L. (2008), Data fusion methods for integrating data-driven hydrological models, in *Quantitative Information Fusion for Hydrological Sciences %V 79 Studies in Computational Intelligence*, edited by X. Cai, and T.-C. Jim Yeh, pp. 1–18, Springer-Verlag, Berlin Heidelberg, doi:10.1007/978-3-540-75384-1.
Seibert, J., and B. L. McGlynn (2007), A new triangular multiple flow direction algorithm for computing upslope areas from gridded digital elevation models, *Water Resour. Res.*, *43*, W04501, doi:10.1029/2006WR005128.
Singh, N. K. (2015), Hydrological and biogeochemical processes in forested headwater catchments of the southern Appalachians, PhD dissertation, N. C. State Univ., Raleigh.
Sklash, M. G., and R. N. Farvolden (1979), The role of groundwater in storm runoff, *J. Hydrol.*, *43*, 45–65.
Soulsby, C., C. Birkel, J. Geris, J. Dick, C. Tunaley, and D. Tetzlaff (2015), Stream water age distributions controlled by storage dynamics and nonlinear hydrologic connectivity: Modeling with high-resolution isotope data, *Water Resour. Res.*, *51*, 7759–7776, doi:10.1002/2015WR017888.
Swank W. T., and J. E. Douglass (1974), Streamflow greatly reduced by converting deciduous hardwood stands to pine, *Science*, *185*(4154), 857–859.
Swift, L. W., G. B. Cunningham, and J. E. Douglas (1988), Climatology and hydrology, in *Forest Hydrology and Ecology at Coweeta*, W. T. Swank and D. A. Crossley, pp. 1–469, Springer, N. Y.
Taylor, J. R. (1982), *An Introduction to Error Analysis: The Study of Uncertainties in Physical Measurements*, Univ. Sci. Books, Mill Valley, Calif.
Tekleab, S., J. Wenninger, and S. Uhlenbrook (2014), Characterisation of stable isotopes to identify residence times and runoff components in two meso-scale catchments in the Abay/Upper Blue Nile basin, Ethiopia, *Hydrol. Earth Syst. Sci.*, *18*(6), 2415–2431.
Tetzlaff, D., and C. Soulsby (2008), Sources of baseflow in larger catchments––Using tracers to develop a holistic understanding of runoff generation, *J. Hydrol.*, *359*, 287–302.
Tetzlaff, D., J. Seibert, K. J. McGuire, H. Laudon, D. A. Burns, S. M. Dunn, and C. Soulsby (2009), How does landscape structure influence catchment transit time across different geomorphic provinces?, *Hydrol. Processes*, *23*(6), 945–953.
Tetzlaff, D., C. Soulsby, M. Hrachowitz, and M. Speed (2011), Relative influence of upland and lowland headwaters on the isotope hydrology and transit times of larger catchments. *J. Hydrol.*, *400*(3), 438–447.
Tetzlaff, D., C. Birkel, J. Dick, and C. Soulsby (2014), Storage dynamics in hydropedological units control hillslope connectivity, runoff generation and the evolution of catchment transit time distributions. *Water Resour. Res.*, *50*, 969–985, doi:10.1002/2013WR014147.
Tetzlaff, D., J. Buttle, S. K. Carey, K. McGuire, H. Laudon, and C. Soulsby (2015), Tracer-based assessment of flow paths, storage and runoff generation in northern catchments: A review, *Hydrol. Processes*, *29*, 3475–3490, doi:10.1002/hyp.10412.
Weiler, M., B. L. McGlynn, K. J. McGuire, and J. J. McDonnell (2003), How does rainfall become runoff? A combined tracer and hydrologic transfer function approach, *Water Resour. Res.*, *39*(11), 1315, doi:10.1029/2003WR002331.